Ray dynamics in long-range deep ocean sound propagation

Michael G. Brown
Rosenstiel School of Marine and Atmospheric Science, University of Miami, Miami, Florida 33149

John A. Colosi
Woods Hole Oceanographic Institution, Woods Hole, Massachusetts 02543

Steven Tomsovic
Department of Physics, Washington State University, Pullman, Washington 99164

Anatoly L. Virovlyansky
Institute of Applied Physics, Russian Academy of Science, 6003600 Nizhny Novgorod, Russia

Michael A. Wolfson
Applied Physics Laboratory, University of Washington, Seattle, Washington 98105

George M. Zaslavsky
Courant Institute of Mathematical Sciences, New York University, New York, New York 10012

(Received 17 September 2001; revised 2 December 2002; accepted 30 January 2003)

Recent results relating to ray dynamics in ocean acoustics are reviewed. Attention is focused on long-range propagation in deep ocean environments. For this class of problems, the ray equations may be simplified by making use of a one-way formulation in which the range variable appears as the independent (timelike) variable. Topics discussed include integrable and nonintegrable ray systems, action-angle variables, nonlinear resonances and the KAM theorem, ray chaos, Lyapunov exponents, predictability, nondegeneracy violation, ray intensity statistics, semiclassical breakdown, wave chaos, and the connection between ray chaos and mode coupling. The Hamiltonian structure of the ray equations plays an important role in all of these topics. © *2003 Acoustical Society of America.* [DOI: 10.1121/1.1563670]

PACS numbers: 43.30.Cq, 43.30.Re, 43.30.Qd [DLB]

I. INTRODUCTION

The chaotic dynamics of ray trajectories in ocean acoustics have been explored in a number of recent publications.[1–17] The purpose of the present paper is to provide a review of results relating to this topic. Our exposition is brief but is intended to be self-contained. We introduce a sequence of ray-based simplifications to the mathematical description of underwater sound propagation in order to get a more complete and clear understanding of the underlying propagation physics, especially in range-dependent environments. We consider these simplifications as the starting point of developing a quantitative theory. It is our opinion that even full wave simulations cannot be used effectively without some understanding of the material described in this paper.

To make our discussion more concrete, we focus our attention on long-range propagation in deep ocean conditions. Theoretical results are emphasized, but with an eye toward analyzing measurements. For this reason considerable attention is paid to results that can be applied in the presence of complicated (nonperiodic) range-dependent ocean structure. In a separate paper many of the results presented and discussed here will be applied to the analysis of a particular data set.

In the next section we review important preliminary material. First, we introduce ray-based solutions to the Helmholtz equation. We then introduce the one-way form of the ray equations and the standard parabolic approximation. Finally, the motion of rays in a range-independent environment is discussed. For this class of problems the ray equations are integrable and the ray trajectories are most naturally described using action-angle variables. In anticipation of the material that follows, the action-angle formalism is introduced.

Section III focuses on the behavior of rays in range-dependent environments, i.e., on nonintegrable ray systems. The action-angle formalism is used here to introduce nonlinear resonances and the KAM theorem. The notion of ray chaos is discussed, as are Lyapunov exponents. Our discussion of the (well known) limitations on the predictability of isolated chaotic trajectories is complemented by a discussion of the (generally unappreciated) stability of families of chaotic trajectories. Also in this section we discuss an important connection between the background sound speed structure and ray stability.

In Sec. IV we discuss ray intensity statistics and related topics, including the distribution of finite range estimates of Lyapunov exponents. The results presented here were first described in the analysis of an idealized underwater acoustic problem, but have since been encountered in other applications. Problems associated with the important task of connecting ray intensity statistics to finite frequency wave field intensity statistics are discussed.

In Sec. V, we provide a more general, but brief, discussion of ''wave chaos''—the study of wave systems that, in the ray limit, exhibit chaotic motion. This topic falls slightly

outside the bounds of providing a review of ray dynamics, but is too important to omit. Strong results relating to this topic are dificult to obtain. Much of our discussion focuses on the question of whether semiclassical (ray-based) wave field representations break down at the so-called Ehrenfest range, which scales as $\ln(\overline{f})$ where $\overline{f}$ is the appropriately nondimensionalized wave frequency.

In Sec. VI, we describe the connection between ray chaos and mode coupling. This work builds on well-known results on ray-mode duality. The results described here provide a promising means of attacking the wave chaos problem inasmuch as finite frequency effects are built into the modal description of the wave field.

In the final section, we briefly discuss two issues. First, we discuss the principal shortcoming of our current knowledge—our relatively poor understanding of the wave chaos problem. Second, we discuss the manner in which ideas relating to deterministic chaos complement and/or conflict with more traditional ideas relating to the study of wave propagation in random media.

II. PRELIMINARY RESULTS

This section provides background material that is necessary to understand the material that is presented in the sections that follow. Starting with the Helmholtz equation we introduce the ray equations and their one-way form, the standard parabolic approximation, and the action-angle description of ray motion in range-independent environments.

A. Waves and rays

Fixed-frequency (cw) acoustic wave fields satisfy the Helmholtz equation,

$$\nabla^2 u + \sigma^2 c^{-2}(\mathbf{r}) u = 0, \tag{1}$$

where u is the acoustic pressure, $\sigma = 2\pi f$ is the angular frequency of the wave field, and $c(\mathbf{r})$ is the sound speed. We consider propagation in a vertical plane $\mathbf{r} = (z,r)$ where z is depth and r is range; the Laplacian operator in (1) is $\nabla^2 = \partial^2/\partial z^2 + \partial^2/\partial r^2$. For large kr, where $k = \sigma/c$, azimuthal spreading of sound generated by a point source can be accounted for by multiplying u by $r^{-1/2}$ if a flat Earth model is assumed, or $(r_e \sin(r/r_e))^{-1/2}$, where r_e is the radius of the Earth, if a spherical Earth model is assumed. The so-called short wave approximation can be used when

$$\sigma \gg |\nabla c|, \tag{2}$$

i.e., when the acoustic wavelength $2\pi/k$ is smaller than all length scales that characterize variations in c. Under such conditions the solution to (1) can be written as a sum of terms, each representing a locally plane wave,

$$u(\mathbf{r};\sigma) = \sum_j A_j(\mathbf{r}) e^{i\sigma T_j(\mathbf{r})}. \tag{3}$$

Substitution of the geometric ansatz (3) into the Helmholtz equation (1) gives, after collecting terms in descending powers of σ, the eikonal equation,

$$(\nabla T)^2 = c^{-2}, \tag{4}$$

and the transport equation,

$$\nabla(A^2 \nabla T) = 0. \tag{5}$$

For notational simplicity we have dropped the subscript j on T and A in (4) and (5). The solution to (4) can be reduced to the solution to the ray equations,

$$\frac{d\mathbf{r}}{d\tau} = \frac{\partial \mathcal{H}}{\partial \mathbf{p}}, \quad \frac{d\mathbf{p}}{d\tau} = -\frac{\partial \mathcal{H}}{\partial \mathbf{r}}, \tag{6}$$

and

$$\frac{dT}{d\tau} = \mathcal{L} = \mathbf{p} \cdot \frac{d\mathbf{r}}{d\tau} - \mathcal{H}, \tag{7}$$

where $\mathbf{p} = \nabla T$ is the ray slowness (also referred to as the momentum) vector and

$$\mathcal{H}(\mathbf{p},\mathbf{r}) = \tfrac{1}{2}(\mathbf{p}^2 - c^{-2}(\mathbf{r})) = 0. \tag{8}$$

The independent (timelike) variable τ satisfies $d\tau/dl = c$ where $dl = |d\mathbf{r}|$, and $d\mathcal{H}/d\tau = 0$. The sum in (3) is over all ray paths $z(r)$ that connect the source at $(z_0,0)$ and the receiver at (z,r). The ray equations (6)–(8) are seen to have Hamiltonian form, which allows many well-known results to be applied to the acoustic problem in the short wave limit. Equations (6)–(8) describe the so-called optical-mechanical analogy of wave propagation in the short wave limit.

For guided wave propagation in the direction of increasing r, the variable r can be used as the independent (timelike) variable and Eqs. (6)–(8) may be rewritten

$$\frac{dz}{dr} = \frac{\partial H}{\partial p}, \quad \frac{dp}{dr} = -\frac{\partial H}{\partial z}, \tag{9}$$

and

$$\frac{dT}{dr} = L = p\frac{dz}{dr} - H, \tag{10}$$

where $p = \partial T/\partial z$ is the z-component of the slowness vector,

$$H(p,z,r) = -\sqrt{c^{-2}(z,r) - p^2} \tag{11}$$

is minus the r-component of the slowness vector, and $dH/dr = \partial H/\partial r$. These are the so-called one-way ray equations. The formal condition for the validity of reducing the two-way ray equations (6)–(8) to the one-way ray equations (9)–(11) is that $dr/d\tau > 0$ following all rays of interest; see, e.g., Ref. 9. All subsequent analysis is based on the one-way ray equations (or a parabolic approximation to these equations, as described below), rather than the slightly more general Eqs. (6)–(8). Ray angles are defined by the condition $dz/dr = \tan\varphi$ where φ is measured relative to the horizontal. Using (9) and (11) this reduces to $cp = \sin\varphi$. An immediate consequence of Eqs. (9), independent of the form of $H(p,z,r)$, is $\partial(dz/dr)/\partial z + \partial(dp/dr)/\partial p = 0$. This is a statement of Liouville's theorem, expressing the incompressibility of flow in phase space (p,z).

The transport equation (5) can be reduced to a statement of constancy of energy flux in ray tubes. In a notation appropriate for use with the one-way ray equations, the solution to the transport equation, assuming a point source, for the jth eigenray can be written

$$A_j(z,r)=A_{0j}|q_{21}|_j^{-1/2}e^{-i\mu_j\pi/2}. \tag{12}$$

The matrix element q_{21}, defined below, describes the spreading of an infinitesimal ray bundle. At any fixed r, one has

$$\begin{pmatrix}\delta p\\ \delta z\end{pmatrix}=Q\begin{pmatrix}\delta p_0\\ \delta z_0\end{pmatrix}, \tag{13}$$

where the stability matrix

$$Q=\begin{pmatrix}q_{11} & q_{12}\\ q_{21} & q_{22}\end{pmatrix}=\begin{pmatrix}\left.\frac{\partial p}{\partial p_0}\right|_{z_0} & \left.\frac{\partial p}{\partial z_0}\right|_{p_0}\\ \left.\frac{\partial z}{\partial p_0}\right|_{z_0} & \left.\frac{\partial z}{\partial z_0}\right|_{p_0}\end{pmatrix}. \tag{14}$$

Elements of this matrix evolve according to

$$\frac{d}{dr}Q=KQ, \tag{15}$$

where Q at $r=0$ is the identity matrix, and

$$K=\begin{pmatrix}-\frac{\partial^2 H}{\partial z\partial p} & -\frac{\partial^2 H}{\partial z^2}\\ \frac{\partial^2 H}{\partial p^2} & \frac{\partial^2 H}{\partial z\partial p}\end{pmatrix}. \tag{16}$$

At caustics q_{21} vanishes and the Maslov index μ advances by one unit. (For waves propagating in three space dimensions, advances by two units are possible.) At these points diffractive corrections to (12) must be applied. The normalization factor A_{0j} is chosen in such a way that close to the source (12) matches the Green's function for the corresponding wave equation, (1) or a parabolic approximation to the one-way form of this equation. (A_{0j} is different for Helmholtz equation and parabolic equation rays; this small difference is of no consequence in any of the results presented below.) Ray intensity statistics are discussed in detail in Sec. IV.

B. The parabolic approximation

The standard parabolic wave equation is

$$-\frac{i}{\sigma}\frac{\partial\Psi}{\partial r}=\left(\frac{c_0}{2\sigma^2}\frac{\partial^2}{\partial z^2}-U(z,r)\right)\Psi, \tag{17}$$

where $u(z,r)\approx\exp(ik_0r)\Psi(z,r)$, $k_0=\sigma/c_0$,

$$U(z,r)=\frac{1}{2c_0}\left(1-\frac{c_0^2}{c^2(z,r)}\right), \tag{18}$$

and c_0 is a reference sound speed. The corresponding ray equations are (9) and (10) with $H(p,z,r)$ replaced by

$$H_{PE}(p,z,r)=\frac{c_0}{2}p^2+U(z,r). \tag{19}$$

Ray angles satisfy $c_0p=\tan\varphi$. The parabolic approximation is valid when ray angles are small and deviations of $c(z,r)$ from c_0 are small. The parabolic wave equation (17) coincides with the Schrödinger equation with r playing the role of time and σ^{-1} playing the role of Planck's constant $\hbar$. [Note that $\hbar/t$ and $(\sigma r)^{-1}$ have the same dimension as the corresponding Hamiltonians.] It is useful to note the analogy between quantum mechanics and acoustics because many tools that have been developed to study quantum chaos, discussed below, can be applied to the study of solutions of (17) or (1) under conditions in which the ray equations, (9) or (6), admit chaotic solutions. In this regard it is noteworthy that there is no direct quantum mechanical counterpart to transient sound fields as these are characterized by the simultaneous presence of a continuum of σ values. (An indirect analog, known as inverse $\hbar$ spectroscopy,[18] has been developed, however.)

C. Integrable ray systems

It is well known that when the sound speed is a function of depth only and the ocean boundaries are surfaces of constant z, the Helmholtz equation (and the parabolic wave equation) admit separable solutions. Under the same conditions the ray equations also admit simple solutions that make use of action-angle variables, and are said to be integrable. The action-angle formalism is important in the material in much of the remainder of the paper, so the essential results are presented here.

When the sound speed is a function of depth only, ray trajectories are periodic; the ray equations (9) can be transformed, via a canonical transformation, to a new set of ray equations in which the Hamiltonian $H(I)$ is a function of the new momentum variable I but is independent of the new generalized coordinate θ. In terms of the action-angle variables (I,θ), ray trajectories are described by the equations

$$\frac{d\theta}{dr}=\frac{\partial H}{\partial I}\equiv\omega(I),\quad \frac{dI}{dr}=-\frac{\partial H}{\partial\theta}=0. \tag{20}$$

The solution to these equations is simply $I=\text{const}$, $\theta(r)=\omega(I)r+\theta(0)$. These equations (and their higher dimensional counterparts) describe motion on a torus. The action variable can be written (see, e.g., Ref. 19) as a function of H (which is constant following each ray trajectory in a range-independent environment),

$$I=\frac{1}{2\pi}\oint dz\,p(H,z)=\frac{1}{\pi}\int_{\check z(H)}^{\hat z(H)}dz\,p(H,z). \tag{21}$$

The integration is over one cycle of the periodic ray trajectory, and at the turning depths $c^{-1}(\check z(H))=c^{-1}(\hat z(H))=-H$. The generating function for the canonical transformation from (p,z) to (I,θ) is

$$G(z,I)=\int^z dz'\,p(H(I),z'), \tag{22}$$

where the $H(I)$ can be obtained by inverting Eq. (21), $p=\partial G(z,I)/\partial z$, and $\theta=\partial G(z,I)/\partial I$.

III. NONINTEGRABLE RAY SYSTEMS

This section is concerned with the behavior of rays in range-dependent environments; under such conditions the ray equations define nonintegrable dynamical systems. The action-angle formalism is used to introduce nonlinear resonances and the KAM theorem. The notion of ray chaos is introduced. Lyapunov exponents and the predictability of

both isolated rays and families of rays are discussed. Also, an important connection between ray stability and the background sound speed profile is discussed.

A. Nonlinear resonances and the KAM theorem

Consider ray motion in an environment consisting of a range-independent sound speed profile to which a small range-dependent perturbation is added. Because of the smallness of the sound speed perturbation, the perturbation to H may be assumed to be additive,

$$H(p,z,r)=H_0(p,z)+\varepsilon H_1(p,z,r). \tag{23}$$

For simplicity, first consider the case where H_1 is a periodic function of r with wavelength $\lambda=2\pi/\Omega$. It is well known (see, e.g., Ref. 4) that for this class of problems canonical perturbation theory fails as nonlinear ray-medium resonances are excited for those rays whose action values I_0 in the unperturbed environment satisfy the condition

$$l\omega(I_0)=m\Omega \tag{24}$$

for any pair of integers, l and m.

A simple analysis (see, for example, Ref. 4) shows that action variables of rays captured into the resonance belong to the interval $I-\Delta I_{\max}<I<I+\Delta I_{\max}$ with

$$\Delta I_{\max}=2\sqrt{\varepsilon\overline{H}_1/|\omega'|}, \tag{25}$$

where $\omega'=d\omega(I)/dI$ at $I=I_0$, and $\overline{H}_1$ is the magnitude of H_1. The quantity $\Delta I_{\max}$ represents the width of the resonance in terms of the action variable. The width of the resonance in terms of spatial frequency can be approximately estimated as

$$\Delta\omega=|\omega'|\Delta I_{\max}/2=\sqrt{\varepsilon\overline{H}_1|\omega'|}. \tag{26}$$

The phenomenon of nonlinear ray medium resonance plays an important role in the emergence of ray chaos. If there are at least two nonlinear resonances centered at spatial frequencies ω and $\omega+\delta\omega$, chaotic motion, according to Chirikov's criterion,[20–22] takes place when the condition

$$\frac{\Delta\omega}{\delta\omega}>1 \tag{27}$$

is satisfied, i.e., when the resonances overlap leading to the stochastic instability of the system.

One might expect that, even for very small ε, all rays are captured into a nearby resonance. This turns out not to be the case. According to the KAM theorem (see, e.g., Ref. 23), for sufficiently small ε some of the tori of the unperturbed system are preserved in the perturbed system, albeit in a slightly distorted form. A condition for the applicability of the KAM theorem is that the nondegeneracy condition $\omega'\neq 0$ must be satisfied. This condition guarantees that resonances are isolated provided ε is sufficiently small. Nondegeneracy violation will be discussed in more detail below.

Realistic sound speed structure in the ocean does not have periodic range dependence, so it is important to consider a larger class of perturbation terms $H_1(p,z,r)$. In Ref. 24 it is shown that the KAM theorem applies to problems for which the perturbation term H_1 consists of a superposition of N components, each of which is periodic in range. N is assumed to be finite but is otherwise unrestricted. The spatial periods need not be commensurable and there may be depth structure associated with each periodic component. Realistic ocean sound speed structure—internal-wave-induced perturbations,[25] for example—can be described by a model of this type. A consequence is that the mixture of chaotic and regular trajectories (discussed below) that characterizes ray motion in environments with periodic range dependence applies to a much larger—and more oceanographically realistic—class of problems.

Because the mixture of chaotic and regular trajectories that characterizes ray motion in environments with periodic range dependence carries over to a much larger class of problems, there is reason to study the former (simpler) problem with the expectation that many of the observed qualitative features carry over to the larger class of problems. The principal advantage of studying ray dynamics in environments with periodic range dependence is that in systems of this type the structure of phase space can be seen by constructing a Poincaré map. To construct such a map, the ray equations (6) and (8) are integrated numerically to give $(p(r),z(r))$. The sequence of points $(p(r_0+n\lambda),z(r_0+n\lambda))$, $n=0,1,2,...$, where λ is the wavelength of the range-dependent sound speed perturbation, is then plotted. A Poincaré map constructed in this fashion is a 2-D slice of the ray motion in the 3-D space (p, z, r mod λ).

For some special problems ray dynamics and associated phase space structures can be studied using an even simpler technique which eliminates the need to numerically trace rays. An example is described in Ref. 5. Here, ray motion in a bilinear model (constant sound speed gradient above and below the sound channel axis) of the deep ocean sound channel was considered. It was shown that when the upper ocean sound speed gradient oscillates periodically in range, successive (separated by one ray cycle) iterates of axial ray angle and range satisfy

$$\begin{aligned}\phi_{n+1}&=\phi_n+\varepsilon[\sin\rho_n+\sin(\rho_n+\phi_n+\varepsilon\sin\rho_n)],\\ \rho_{n+1}&=\rho_n+\phi_n+\varepsilon\sin\rho_n+\gamma\phi_{n+1}.\end{aligned} \tag{28}$$

Here ε is the dimensionless perturbation strength, γ is the ratio of the average upper ocean sound speed gradient g to the fixed lower ocean sound speed gradient, $\phi_n=(4\pi/g\lambda)\varphi_n$ and $\rho_n=(2\pi/\lambda)r_n$. These equations define an area-preserving mapping, $\partial(\phi_{n+1},\rho_{n+1})/\partial(\phi_n,\rho_n)=1$; this condition is a discrete analog of Liouville's theorem. Because of their relative simplicity, area-preserving mappings are widely used to study properties of nonintegrable Hamiltonian systems. Some of these properties will now be described.

B. Ray chaos

Figure 1(a) shows iterates of Eq. (28) for many sets of ray initial conditions in an environment with moderately strong ($\varepsilon=0.15$) range dependence. Phase space is seen to consist of a mixture of regular and chaotic regions, often described as regular islands in a chaotic sea. For much smaller values of ε, chaotic regions occupy only thin isolated

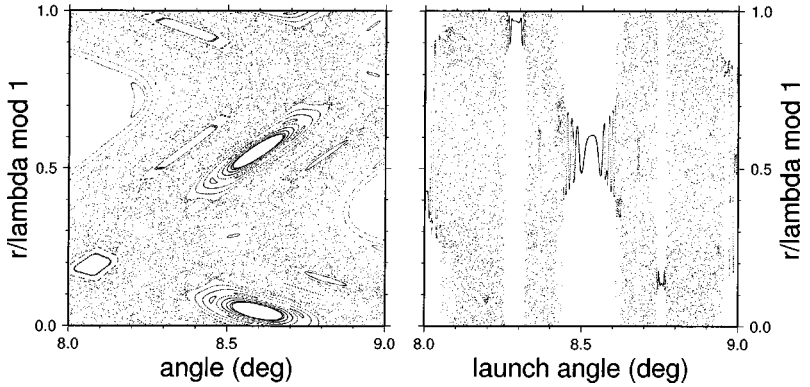

FIG. 1. Numerical simulations based on the area-preserving mapping (28) with $g=1/(30\,\mathrm{km})$, $\lambda=10\,\mathrm{km}$, $\gamma=4$, and $\varepsilon=0.15$. In both plots the ray initial conditions correspond to those of an axial point source at $r=\lambda/2$. Left panel: 500 iterates of the mapping for 50 rays whose launch angles are uniformly distributed between 8° and 9°. Right panel: range after 250 ray cycles (each corresponding to one iteration of the mapping) for 10 000 rays whose launch angles are uniformly distributed between 8° and 9°. In most regions this sampling interval is too large to resolve what should be a smooth function.

bands of phase space. Each such thin chaotic band is associated with an isolated resonance. As ε is increased, the widths of the resonances increase and nearby resonances overlap, leading to an intricate mixture of regular and chaotic regions, as seen in Fig. 1(a). Behavior of this type is typical of systems that are constrained by KAM theory. Figure 1(b) shows a plot of range versus launch angle after 250 ray cycles in the same environment, and using rays emanating from the same fixed point that was used to produce Fig. 1(a). The ray initial conditions used in both Figs. 1(a) and (b) fall on a horizontal line (at $r=\lambda/2$) through the middle of Fig. 1(a). Note that the islands that intersect this line in Fig. 1(a) are readily identifiable in Fig. 1(b). This observation is significant because plots like Fig. 1(b)—ray position versus some continuous ray label—can be constructed in environments with nonperiodic range dependence, providing a simple means of identifying islandlike structures.

At the boundaries of chaotic and regular domains—in Fig. 1(a), for example—are usually invisible cantori. These are Cantor-type invariant sets with fractal structure containing an infinity of holes. Cantori act as partial barriers that inhibit the diffusion of rays. Boundaries of chaotic regions contain small island chains around which the density of points is very high. A common phenomenon is ''stickiness'' of island boundaries; after wandering in an apparently random fashion in phase space, a chaotic trajectory may approach a stable island, and stick to its border for some (possibly long) time, during which it exhibits almost regular behavior.[26] The presence of regular islands in phase space alters the dispersion characteristics of the trajectories that lie in the surrounding chaotic sea.[26] Details depend on the structure of phase space but the phenomenon of anomalous diffusion (mean square displacements of trajectories in phase space obeying scaling laws different than those of a traditional random walk) seems to be generic.

An important property of chaotic trajectories is that they exhibit extreme sensitivity, characterized by a positive Lyapunov exponent,

$$\nu_{\mathrm{L}}=\lim_{r\to\infty}\left(\frac{1}{r}\lim_{\mathcal{D}(0)\to 0}\ln\frac{\mathcal{D}(r)}{\mathcal{D}(0)}\right). \tag{29}$$

Here $\mathcal{D}(r)$ is a measure of the separation between rays at range r. Suitable choices for $\mathcal{D}(r)$ are separations in z or p; another choice is described in Sec. IV. The Kolmogorov–Sinai entropy h_{KS} is closely related to ν_{L}. Loosely speaking, h_{KS} is a measure of information increase following a trajectory; a readable discussion of this topic can be found in Ref. 27. For bounded dynamical systems $h_{\mathrm{KS}}\sim\nu_{\mathrm{L}}$ holds; in open diffusive systems, their difference is proportional to a diffusion constant.[28] A consequence of the extreme sensitivity of chaotic rays is that the number of eigenrays connecting a fixed source and receiver grows exponentially, like $\exp(h_{\mathrm{KS}}r)$, on average in range.[1,9,12] Also, the magnitudes of the variational quantities q_{ij} [see Eq. (14)] can grow exponentially, on average, in range. Reference 17 contains a detailed discussion of this topic. A consequence of this exponential growth is that the amplitudes of chaotic rays [proportional to $|\partial z(r)/\partial p(0)|^{-1/2}$ for (9) or $|\partial\rho_n/\partial\phi_0|^{-1/2}$ for (28), assuming a point source] decay exponentially, on average, in range. Note, however, that for moderate to large r or n (measured in units of a typical value of ν_L^{-1}), plots of $\partial z(r)/\partial p(0)$ vs $p(0)$ (see Fig. 5) or $\partial\rho_n/\partial\phi_0$ vs ϕ_0 (see Fig. 1) have fractallike structure when both chaotic and regular trajectories are present.

Another consequence of extreme sensitivity of chaotic rays is that deterministic predictions using finite precision numerical arithmetic is limited to ranges less than some threshhold (which is proportional to N_b/ν_L where N_b is the number of bits used to specify the mantissa of floating point numbers). This limitation on one's ability to make deterministic predictions of chaotic ray trajectories at long range is tempered by two related factors. First, the shadowing lemma[27] guarantees that, for a large class of problems, numerically computed chaotic trajectories at long range correspond to trajectories of rays whose initial conditions are close to the specified values but are generally unknown. Second, it is easy to verify that statistical properties of discretely sampled distributions of chaotic rays (occupying, for example, a small but finite area in phase space at $r=0$) evolve in a way that does not exhibit extreme sensitivity.

A somewhat stronger form of stability of distributions of chaotic rays is illustrated in Fig. 2. In phase space an aperture-limited compact source is represented as a line segment at constant depth $z=z_0$ bounded by limiting values of p_0; this is an example of a Lagrangian manifold. Each point on such a manifold evolves in r according to the ray equations (9). As a Lagrangian manifold evolves, it gets stretched and folded, but does so without breaking or intersecting itself (owing to phase space area preservation). Figure 2 illustrates one aspect of a phenomenon that can be termed manifold

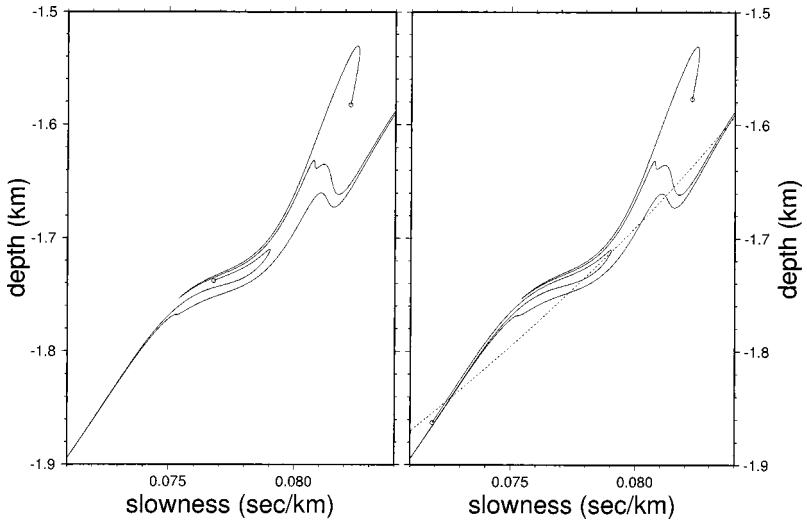

FIG. 2. Left panel: segment of a Lagrangian manifold for a fan of rays with $z(0)=-1.100$ km, $8.575° \leqslant \theta(0) \leqslant 8.625°$ at $r=500$ km in the background environment shown in Fig. 3 with an internal-wave-induced sound speed perturbation superimposed. Right panel: segment of a Lagrangian manifold for a fan of rays with $z(0)=-1.101$ km, $8.575° \leqslant \theta(0) \leqslant 8.625°$ at $r=500$ km in the same environment. The endpoints of both Lagrangian manifolds are marked with small open circles. In both panels, portions of the manifold segments, consisting of long thin tendrils, extend beyond the plot boundaries. The dashed curve in the right panel is a portion of a surface $I=$const.

stability. In this figure two Lagrangian manifolds with slightly different initial conditions are plotted in phase space at a fixed range, $r=500$ km. Each manifold has initial conditions $z=z_0$ (a constant), $8.575° \leqslant \theta_0 \leqslant 8.625°$. For one of the manifolds $z_0=1.100$ km; for the other $z_0=1.101$ km. Both manifolds evolved in the same environment, which is described below. In this environment almost all trajectories evolve chaotically, which leads to exponential growth in range of the length of each manifold. The combination of chaotic ray motion and the small difference in initial manifold depth might lead one to expect that the two manifolds should evolve very differently. Figure 2 shows clearly, however, that they have not. This can be explained by noting that phase space area is preserved. Because of this constraint, the exponential stretching of each manifold is balanced by an exponential contraction of phase space in the transverse direction. This contraction causes the two manifolds to get squeezed closer to one another. Note, however, that, in general, points on the two manifolds with the same value of θ_0 do not lie close to one another. Loosely speaking, the two manifolds have slid relative to one another while being stretched, folded, and squeezed toward one another. Trajectories with nearby initial conditions will also be squeezed toward the same locus of points. Thus, although individual trajectories exhibit extreme sensitivity under chaotic conditions, the associated exponential contraction of phase space elements imparts a surprisingly strong form of stability on continuous distributions of trajectories. The impact of manifold stability on wave field evolution and stability is considered in Ref. 29.

The environment used to produce Fig. 2 is also used in subsequent numerical work. It consists of a range-independent background profile, shown in Fig. 3, on which an internal-wave-induced sound speed perturbation field is superimposed. The background profile is a Munk[30] profile modified in the upper ocean, $c(z)=c_0(1+\varepsilon(\exp\eta-\eta-1))+c_u(z)$, with $c_0=1.49$ km/s, $\epsilon=0.0057$, $\eta=2(z-z_a)/B$, $B=1$ km, $z_a=-1.1$ km, and $c_u(z)=\delta\sin^2(\pi(z-z_a)/z_a)$ for $z>z_a$ with $\delta=0.018$ km/s. The internal-wave-induced sound speed perturbation was computed using Eq. (19) of Ref. 25 with $y=t=0$, i.e., a frozen vertical slice of the internal wave field was assumed. An exponential buoyancy frequency $N(z)=N_0\exp(z/B)$ (note that depths z are negative with $z=0$ at the sea surface) with $N_0=6$ cycles/hour was used. The dimensionless strength parameters E and μ were taken to be 6.3×10^{-5} and 17.3, respectively. Numerically, a 2^{14} point FFT was used with $\Delta k_x=2\pi/1638.4$ km, $k_{x,\max}=2\pi/1$ km and $j_{\max}=30$. It should be noted that this perturbation field is highly structured and fairly realistically describes typical deep ocean environments. Also, the assumed background profile is similar to profiles found in much of the North Atlantic Ocean.

The unpredictability associated with ray chaos is, of course, partially mitigated by finite frequency smoothing effects. This will be discussed in Sec. V. We have seen, however, that even without accounting for finite frequency smoothing, loss of predictability associated with ray chaos is less severe than might be expected due to the constraining influences of Liouville's theorem, and, for a large class of

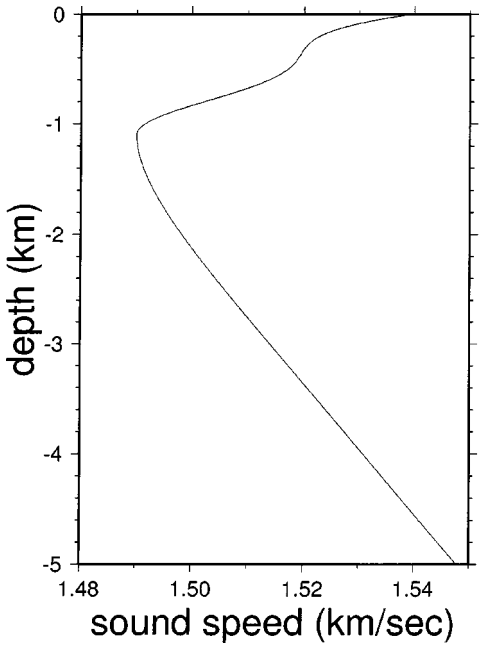

FIG. 3. Background sound speed profile used to produce Figs. 2, 4, and 5.

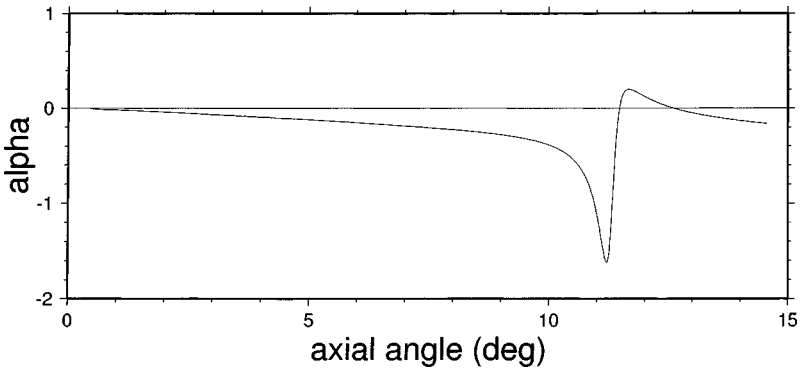

FIG. 4. Stability parameter α versus axial ray angle in the environment shown in Fig. 3.

problems, the coexistance of chaotic and nonchaotic trajectories. Because of these influences chaotic ray systems have more subtle dynamics than purely stochastic systems. Systems of the latter type arise—in studies of wave propagation in random media, for example—when sound speed perturbations to a homogeneous background are assumed to be delta correlated. The topic described in the following subsection is an example of a topic that fits naturally into a dynamical systems framework, but not into a purely stochastic framework.

C. Ray stability and ω'

Recall from Sec. III A that in order for the KAM theorem to apply the nondegeneracy condition,

$$\frac{d\omega}{dI} \neq 0, \tag{30}$$

must be satisfied in the background (range-independent) environment. Systems in which the nondegeneracy condition is violated may admit chaotic solutions, but such systems are characterized by the presence of a stochastic web[31] (or perhaps some other structure), rather than the regular island/chaotic sea mixture that characterizes chaotic systems that are constrained by KAM theory. Note, in addition, that Eqs. (26) and (27) show that $\omega' = d\omega/dI$ also plays an important role in systems that are constrained by KAM theory; if the perturbation strength $\varepsilon \overline{H}_1$ is fixed, then rays are expected to become increasingly chaotic as $|\omega'|$ increases because as $|\omega'|$ increases the number of overlapping resonances should increase. These observations suggest that ray behavior should be influenced by the background sound speed structure via the quantity ω'. Numerical evidence, including an example described below, confirms this expectation.

It is convenient to introduce, following Zaslavsky,[32] the dimensionless stability parameter

$$\alpha = \frac{I}{\omega}\frac{d\omega}{dI}. \tag{31}$$

The stability parameter $\alpha(I)$ is a property of a range-independent environment $c(z)$ and is a function of the action variable I—or some equivalent ray label such as horizontal ray slowness p_r or axial ray angle. $\alpha(I)$ can be computed from more familiar ray quantities. The angular frequency $\omega = 2\pi/R$ where R is the ray cycle distance. For Helmholtz equation rays

$$R(p_r) = 2p_r \int_{\check{z}}^{\hat{z}} \frac{dz}{(c^{-2}(z) - p_r^2)^{1/2}}, \tag{32}$$

where p_r is the r-component of the ray slowness vector, which is constant following a ray trajectory in a range-independent environment. The upper turning depth of a ray $\hat{z}(p_r)$ satisfies $c(\hat{z}(p_r)) = p_r^{-1}$, and similarly for the lower turning depth $\check{z}(p_r)$. Also, $cp_r = \cos\varphi$. The action can be written

$$I(p_r) = \frac{1}{\pi}\int_{\check{z}}^{\hat{z}} dz\,(c^{-2}(z) - p_r^2)^{1/2}. \tag{33}$$

Because $2\pi dI/dp_r = -R(p_r)$, $\alpha = (2\pi I/R^2)dR/dp_r$. This expression for α is convenient to evaluate numerically. A deep-ocean α-curve, corresponding to the sound speed profile shown in Fig. 3, is shown in Fig. 4.

In Fig. 4 zeros of α—where the nondegeneracy condition (30) is violated—are seen to be isolated. Such points are referred to in Ref. 21 as accidental degeneracies, in constast to intrinsic degeneracy where ω' vanishes for all trajectories. Parabolic equation rays in environments in which $U(z)$ is quadratic and Helmholtz equation rays in environments in which $c(z) = c_0 \cosh((z - z_0)/h)$ are intrinsically degenerate. These special problems are not realistic oceanographically. Also, it is worth noting that perturbations to intrinsically degenerate systems often break up the degeneracy, leading to phase space structure that is essentially the same as that seen in nondegenerate systems.[21] Accidental degeneracies, on the other hand, are structurally stable and, as illustrated in Fig. 4, are common in realistic deep ocean α-curves.

Reference 33 presents an extensive set of numerical simulations and some nonrigorous theoretical arguments that complement those given above in an attempt to better understand the connection between ω' and ray stability. The conclusions of that study are that ray stability is largely controlled by $|\omega'|$ and that ray instability (as measured by Lyapunov exponents, for example) increases with increasing $|\omega'|$. These statements are consistent with the argument presented above based on Eqs. (26) and (27). The connection between $|\omega'|$ and ray instability is illustrated by comparing Figs. 4 and 5. Figure 5 shows ray depth at a range of 1000 km as a function of launch angle for an axial source in the environment shown in Fig. 3 on which an internal-wave-induced sound speed perturbation was superimposed. (The internal-wave-induced perturbation used to produce Fig. 5 was identical to that used to produce Fig. 2 apart from a

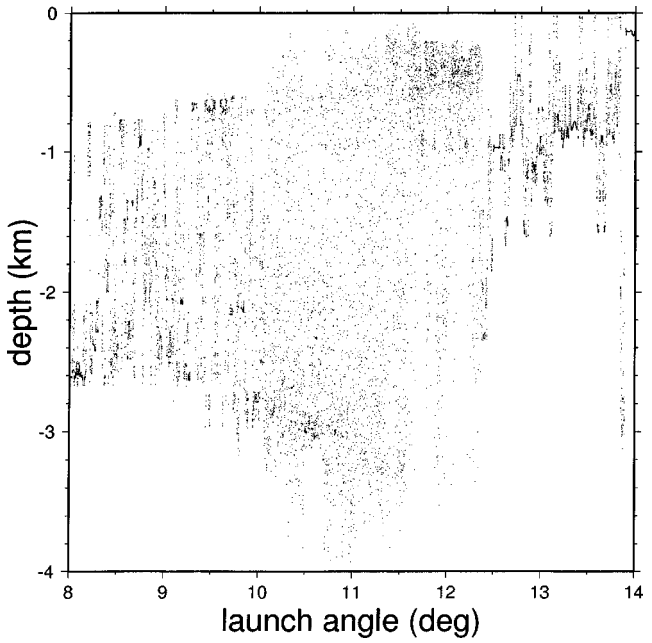

FIG. 5. Ray depth versus launch angle for an axial source at a range of 1000 km in the background environment shown in Fig. 3 with an internal-wave-induced sound speed perturbation superimposed. In most regions the sampling interval ($\Delta\theta_0 = 0.0005°$) is too large to resolve what should be a smooth function.

factor of 2 reduction in the strength parameter E.) In Fig. 5 it is seen that rays in the 10° to 12° band are evidently much less stable than those outside this band. Outside of this band there is evidence of apparently nonchaotic islandlike structures (compare to Fig. 1); inside this band, there is no indication—at the resolution shown, at least—of the presence of such structures. Note that the unstable band of rays in Fig. 5 overlies the band of rays near the peak in $|\alpha|$, corresponding to axial ray angles near 11.1°, seen in Fig. 4. The unstable band of rays seen in Fig. 5 is broader than the peak in $|\alpha|$ seen in Fig. 4. This is because rays whose initial axial angle falls slightly outside the unstable band get scattered into the unstable band. Neither Fig. 5 nor the numerical simulations shown in Ref. 33 show any evidence of structures resembling stochastic webs near isolated zeros of $|\omega'|$. Presumably this is due, in part at least, to the complexity of the internal-wave-induced sound speed perturbations that were used in the simulations, but this issue deserves to be studied more systematically.

Because significant variations in $|\omega'|$ are common in realistic models of (background) ocean structure, we expect the qualitative behavior exhibited in Figs. 4 and 5 to be fairly common in ocean acoustics. Reference 34 first investigated the connection between ray stability and the sound speed structure. Later Simmen *et al.*[14] showed that, for identical sound speed perturbation fields, characteristics of ray stability versus launch angle curves depend strongly on the background sound speed profile. Variations in $|\omega'|$ are a likely cause of the latter finding.

IV. RAY INTENSITY STATISTICS

Ray intensity distributions are discussed in this section. There are two principal reasons for investigating this topic. First, ray intensity distributions are a useful diagnostic tool to study and quantify ray dynamics,[17] especially in environments with nonperiodic range dependence where Poincaré maps cannot be constructed. Second, one expects—on the basis of the local plane wave expansion (3)—that a useful starting point for understanding wave field intensity statistics is understanding ray intensity statistics. We emphasize that gaining an understanding of ray intensity statistics is only the first step in this process, as diffraction and interference effects must be accounted for in making the transition to wave field intensity statistics. These complications will be discussed in more detail in the section that follows. The material presented here builds on the material presented in Sec. II A that relates to ray intensities.

We shall confine our attention to a discussion of ray intensity statistics in a simple idealized ocean model. A more detailed account of the results presented here can be found in Ref. 17. Some related results for the same idealized problem are presented in Ref. 16. The model consists of an unbounded homogeneous background on which an isotropic, single scale (described by a Gaussian spectrum) random perturbation is superimposed. In this idealized problem, which is the basis of much work on the study of wave propagation in random media,[35] all rays are chaotic. It should not be expected that all of the properties of ray intensity distributions in our idealized problem carry over to long-range deep ocean propagation conditions, which are characterized by the presence of a background sound channel on which strongly inhomogeneous and isotropic internal-wave-induced sound speed fluctuations with a power-law spectrum are superimposed. In spite of the idealized nature of the problem considered here, there is ample justification for studying this problem. First, this simple problem has surprisingly rich structure that must be understood before more complicated problems can be successfully attacked. Second, the results presented are expected to comprise a limiting case of those that apply to more complicated problems. And third, preliminary results suggest that many of the results presented here apply generally to systems that are far from integrable. This topic will be discussed in more detail elsewhere.

It is also worth mentioning that the results presented here are expected to apply to other fields, as well. Twinkling starlight is a familiar example, but far more exotic systems with the same dynamical foundation exist. Two such examples are the gravitational bending of light passing through galaxy clusters,[36] and quantum mechanical waves associated with the transport of low-temperature conduction electrons through semiconductor materials.[37] Recent experiments of this latter system show the electron transport breaking up into coherent channels that follow bundles of classical rays that are only weakly unstable in spite of the semiconductor acting as a random medium.[38] This is a manifestation of the remaining stable and nearly-stable rays mentioned in Sec. III in connection with the KAM theorem; such rays will show up again later in this section.

Ray stability analysis relies on the stability matrix Q defined in Eq. (13) from which a great deal of information can be deduced. The stability matrix describes the behavior of all rays that remain within an infinitesimal neighborhood

of a reference ray over the course of its propagation. As seen in Eq. (12), geometric amplitudes for a point source are controlled by the matrix element q_{21}; for a plane wave initial condition q_{22} is the relevant quantity. For pedagogical purposes, however, it is simpler to consider the trace of the matrix; for chaotic rays, its exponential rate of increase and gross statistical properties are the same as those of any of the Q matrix elements. Since Q is diagonalizable by a linear, similarity transformation

$$\Lambda = LQL^{-1} \Rightarrow \begin{pmatrix} \lambda & 0 \\ 0 & \lambda^{-1} \end{pmatrix}, \tag{34}$$

its trace is an invariant equal to the sum of the eigenvalues. The last form applies to systems with a single degree of freedom because the determinant is unity. Three distinct cases may arise. The first is $|\mathrm{Tr}(Q)|<2$ which is linked to stable motion, and it is customary to denote $\lambda = \exp(i\theta r)$. The second case is $|\mathrm{Tr}(Q)|=2$, and it is often called marginally stable because it is the boundary case between stable and unstable motion. The third case represents unstable motion, and is characterized by $|\mathrm{Tr}(Q)|>2$. There it is customary to denote $\lambda = \pm\exp(\nu r)$ where ν is positive and real.

In systems that are far from integrable, the vast majority of rays fall into this last category. Their largest Lyapunov exponent takes on an alternative form to Eq. (29), which can be expressed as

$$\nu_{\mathrm{L}} \equiv \lim_{r\to\infty} \frac{\ln|\mathrm{Tr}(Q)|}{r}. \tag{35}$$

For unstable trajectories we may approximate $\mathrm{Tr}(Q)=\lambda + 1/\lambda \approx \lambda$ with little inaccuracy. In the system described in Refs. 16 and 17 ν_{L} is the same for all rays. But finite range estimates of ν_{L}, sometimes referred to as stability exponents,

$$\nu = \frac{\ln|\mathrm{Tr}(Q)|}{r}, \tag{36}$$

generally differ from ν_{L}. If one introduces an ensemble of potentials U, each member of which generates a dynamical system with the same ν_{L}, then the ensemble average of ν converges to ν_{L}, except at very short range. The statistical properties of ν will be described in more detail below. We note here, however, that the fluctuations in ν are very important because even modest fluctuations in ν produce immense fluctuations in $\mathrm{Tr}(Q)$ which imply similar fluctuations in q_{21}. These large fluctuations in q_{21} are important because in a chaotic system at long range the number of eigenrays can be enormous, but the wave field may be dominated by a tiny fraction of these whose values of $|q_{21}|$ are small.

An analytic expression for the root mean square exponential rate of increase of $\mathrm{Tr}(Q)$ has been derived using techniques relying on Markovian assumptions:[16]

$$\mathrm{Tr}(Q)_{\mathrm{RMS}} \sim \exp(\nu' r). \tag{37}$$

where

$$\nu' \approx \left(\frac{1}{2} \int_0^\infty d\xi \left\langle \left. \frac{\partial^2 U(z;r-\xi)}{\partial z^2} \right|_{\substack{z=z_0 \\ p=p_0}} \left. \frac{\partial^2 U(z;r)}{\partial z^2} \right|_{\substack{z=z_0 \\ p=p_0}} \right\rangle \right)^{1/3}, \tag{38}$$

and the brackets, $\langle ... \rangle$, denote ensemble averaging over different realizations of the potential U. Numerical evaluation of Eq. (38) for model systems with some realism is usually necessary, but analytic results are available for simplified models such as Gaussian random single scale potentials.

Interestingly, ν' is greater than the Lyapunov exponent, independent of the range involved. In fact, with increasing range it rapidly approaches a constant. The important distinction lies in whether the ensemble averaging occurs before or after taking the natural logarithm. The fluctuations are strong enough that $\nu' > \nu_{\mathrm{L}}$ $(=\langle\nu\rangle)$ or alternatively

$$\frac{\ln\langle|\mathrm{Tr}(Q)|^2\rangle}{2r} > \left\langle \frac{\ln|\mathrm{Tr}(Q)|}{r} \right\rangle \tag{39}$$

for all appreciable r.

In the environment consisting of a homogeneous background on which a single scale Gaussian perturbation is superimposed, the probability density of ν is very nearly (except in the far tails) a Gaussian of mean ν_{L} and variance

$$\sigma_\nu^2 = \frac{\nu' - \nu_{\mathrm{L}}}{r}. \tag{40}$$

This distribution has also been observed in numerical simulations based on more realistic ocean models. This topic will be discussed in more detail elsewhere. Numerical calculations also suggest that the Gaussian statistics are obtained for each realization of the random medium just by choosing different initial conditions; i.e., an ensemble of media is not necessary. A Gaussian density for ν implies a lognormal density for $|\mathrm{Tr}(Q)|$ whose parameters are fixed by the Gaussian density's mean and variance. A property of lognormal densities is that any power of the variable also has a lognormal density. Thus, $|\mathrm{Tr}(Q)|^\gamma$ has a lognormal density as well; $\gamma = -\frac{1}{2}$ relates to the semiclassical approximation. However, note that depending on the value of γ, the lognormal density may fail as an approximation less far out in the tails.

In the limit of long range, the fluctuations in $|\mathrm{Tr}(Q)|$ grow without bound despite ν approaching ν_{L} for every ray. Just as there are highly unstable rays, there are also rays which are stable or nearly stable. The lognormal density gives a prediction for what approximate proportion is left for a given propagation range. Asymptotically, the proportion of nearly stable rays, whose stability exponent is less than some small value ν_c, decreases exponentially with range as $(a_0/4\pi r)^{1/2}\exp(-r/a_0)$ where $a_0 = 2(\nu' - \nu_{\mathrm{L}})/(\nu_{\mathrm{L}} - \nu_c)^2$.

The connection to the statistical behavior of wave field intensities arising from the lognormal density of classical ray intensities is not yet understood. There are a number of subtleties. To begin with, for long ranges of propagation, the most naive picture of semiclassical theory leads to the expectation that the wave field is made up of an extremely large number of extremely small contributions. On average, if diffusive growth in phase space is neglected, the growth of the number of eigenrays and the decay of a typical ray intensity

(squared amplitude) should occur at the same exponential rate. If this is true, energy conservation considerations dictate that at long range the constituent ray arrivals have effectively random phases. In other words, a set of N random, uncorrelated numbers of scale $N^{-1/2}$ maintains an order unity summation as $N \to \infty$. Chaotic dynamics is deterministic, and at best, the semiclassical phases generated by the dynamics are pseudo-random at long range. For shorter ranges, correlations amongst the magnitudes and phases could alter the statistical predictions. These correlations remain to be studied. Furthermore, the possibility mentioned earlier that one or few very strong terms at short range could dominate the sum increases the difficulty in finding a unique approach to an asymptotic statistical limit.

A second difficulty is that the lognormal distribution has long tails, indicative of a broad range of fluctuations. The lognormal distribution of intensities y has the form $y^{-a_0 \ln y}$ which can be verified to approach zero for large or small y faster than any power of y, but does not decay exponentially. A sum of random numbers chosen from long tailed densities may not approach a standard central theorem limit (the Lorentzian density remains Lorentzian under repeated convolution), or may approach it very slowly. For the ray chaos problem, as the number of eigenrays grows with increasing range, the breadth of the density is also increasing. If the approach to a central limit theorem is slow enough, then it might never be reached under these circumstances; the limiting density still needs to be worked out.

A third, extremely important difficulty is the appearance of caustics. Their number proliferates at the same exponential rate for chaotic systems as the number of eigenrays. At the caustics, the semiclassical expressions diverge and introduce infinities. Caustics correspond to the extremely small values of instabilities in the tail of the lognormal density where breakdown of the statistical laws are likely. The lognormal expression does not capture the physics of singularity dominated fluctuations that are characterized by twinkling exponents which depend on the types of caustics present.[39–41] Thus, some incorporation of deviations from lognormality appears to be inescapable. In addition, the presence of exponentially proliferating numbers of caustics calls into question the very relevance of semiclassical methods and their usefulness in predicting the statistical properties of the wave field. This consideration is intimately linked with discussions of the validity of the semiclassical approximation for chaotic systems of which we give an overview in the next section.

A final noteworthy complication arises in the analysis of sound fields produced by a broadband source. Interference must still be accounted for, but only among ray arrivals whose travel times fall within intervals whose duration is the reciprocal bandwidth $(\Delta f)^{-1}$ of the source. This phenomenon is further complicated when pulse shapes and phase shifts at caustics—corresponding to Hilbert transforms in the time domain—are taken into account.

V. WAVE CHAOS

''Wave chaos'' is the study of wave systems that, in the ray limit, exhibit unstable dynamics (i.e., exponential divergence of neighboring rays); the underwater sound propagation problem can be thought of as a wave chaos problem. A completely analogous definition of the phrase ''quantum chaos'' is widely used. These two subjects are similar enough that much, if not most, of the progress in either domain carries readily over into the other; we therefore do not bother to distinguish them here. It turns out that there are significant conceptual difficulties with attempting to associate wave chaos with an unbounded, exponential growth of wave field complexity in the hope that a straightforward generalization of the underlying ray chaos manifests itself. The shorthand explanation of this difficulty is often crudely stated something like ''the finite wavevector (nonzero Planck's constant $\hbar$) smooths over the intricate, fine scale details of the chaotic dynamics, not allowing them to be seen.'' The correspondence principle for chaotic systems, in fact, is quite subtle, and we avoid going into this fascinating subject except for the issue of the breakdown of semiclassical theories which we summarize next.[42] For further details though, we refer the reader to Ref. 43 for a discussion of some aspects of wave chaos in underwater acoustics, and to some recent literature relating to quantum chaos.[44,45]

The aspect of the breakdown of semiclassical theories which interests us most for the purposes of this paper is whether or not it is possible to construct, on solid theoretical ground, a ray-based theory valid beyond where ray chaos has fully developed. If not, ray-based predictions under chaotic conditions that match data in long-range propagation experiments would have to be considered accidental, and not an explanation of the essential physics of the problem. It may turn out that the eventual answer to this question is not unique, and depends upon which quantity one wishes to explain. For example, statistical predictions may be more robust than detailed, pointwise, wave field predictions. On the other hand, if the breakdown occurs on a scale much longer than that of the development of ray chaos, there remains a great deal of theoretical work to be pursued.

There is some hope for optimism in this regard. We begin by distinguishing between two classes of dynamical systems. The first class is that of simple, chaotic systems. Equations (28) define a system of this type. The equations of motion may be deceptively simple to write down, yet the solutions highly complicated, and, for all intents and purposes, analytically intractable (chaotic). The second class has complicated equations in the sense that the medium satisfies many of the criteria of randomness even though it is taken here to be deterministic (we may not know which deterministic realization is given in a particular case). One cannot take for granted the equivalence of the properties of these two classes of systems (chaotic versus random media), but we note that in certain limits there exist a number of common results (such as exponential ray instability with respect to initial conditions).

In simple chaotic systems, about which more is known concerning semiclassical breakdown, we have to be careful to distinguish three levels of dynamics: classical, quantum, and semiclassical. We emphasize that the last level should be distinguished from the classical in that it takes classical information as input, but it actually generates an approximate

construction of the quantum dynamics at the level of wave amplitudes and phases. The distinctions between time-evolving classical and quantum expectation values of operators or classical and quantum probability densities have been studied since the development of quantum mechanics. Those quantities that correspond to each other initially are known to propagate similarly before diverging over a finite time scale called the Ehrenfest time. For simplicity, we shall focus only on the fact that one cannot delay the onset of interference phenomena in the quantum dynamics beyond the Ehrenfest time, and interference is necessarily excluded from the classical dynamics. For chaotic systems, the Ehrenfest time depends logarithmically on $\hbar$,[46] and beyond this time scale one finds all manner of complications such as an exponential proliferation of rays, increasing uncertainty whether the rays can even be calculated, and proliferating caustics in semiclassical theories. There is no debate whether the classical and quantum dynamics diverge beyond the Ehrenfest time (they do by definition); the relevant debate centers upon whether a ray-based, semiclassical theory can surmount these difficulties.

There are various ''flavors'' of semiclassical approximations possible. For example, the Wigner–Weyl calculus or other constructions of pseudo-phase spaces[47] are ideally suited for exhibiting how the classical limit emerges from quantum mechanics in a semiclassical limit, but they are poorly adapted for describing interference phenomena. Indeed, mathematical proofs exist that such phase-space-based semiclassical approximations cannot be extended beyond a logarithmic time scale; see Ref. 48. In this scenario, it can be fruitful to examine smoothed features of the wave field (as opposed to pointwise comparisons), such as can be obtained through the ray-based construction of the coarse-grained Wigner function.[49] However, the development of semiclassical approaches that can be roughly described as time-dependent WKB theory handle interference naturally though multiple stationary phase (saddle point) contributions. This approach has been applied to a number of paradigms of chaos (the bakers map, the stadium, and the kicked rotor) with excellent, numerical results extending well beyond the logarithmic time scale.[50–52] Arguments leading to the expectation that the breakdown time depends algebraically on $\hbar$ have also been presented.[51–53]

Semiclassical breakdown in an idealized, but highly structured, ocean model consisting of a single realization of a ensemble with prescribed statistics has been investigated by Brown and Wolfson. They constructed the full semiclassical approximation using the classical dynamics and a Maslov–Chapman uniformization procedure. In their comparisons, they found the semiclassical approximation appeared to be working quite well beyond the onset of ray chaos.[54] This work and those quoted for simple chaotic systems are claiming that it is possible to extend a semiclassical theory for both chaotic and random media problems beyond a logarithmic time (range) scale, and, thus, that ray-based semiclassical theories are viable candidates purporting to explain the essential physics of wave chaotic dynamical problems.

VI. CHAOS AND MODE COUPLING

In this section the connection between ray chaos and mode coupling is described. The results presented provide a promising means of addressing the wave chaos problem inasmuch as finite frequency effects are built into the modal description of the wave field. The material presented here makes use of the action-angle formalism introduced in Sec. II C. The connection between ray and modal expansions of acoustic wave fields in range-independent environments is well understood (see, e.g., Refs. 55–57) and some generalizations have been derived[58–60] for range-dependent environments. Thus, it should come as no surprise that there is a quantifiable connection between ray chaos and the modal description of the wave field. Some details omitted in our presentation of this material can be found in Refs. 61 and 62. To simplify the presentation somewhat, we make use of a WKB analysis of the parabolic wave equation. Consistent with our use of the parabolic wave equation, the variables $p'=c_0 p$, $H'=c_0 H_{PE}$, $U'=c_0 U$, and $I'=c_0 I$ are used in this section after dropping the primes. Also, $S=c_0 T$ is used in place of T.

The principal result of this section is an approximate analytical expression for mode amplitudes in term of raylike quantities. We discuss how typical features of ray chaos, such as exponential growth (with range) of eigenrays contributing to the field point and coexistence of chaotic and regular ray trajectories, manifest themselves in the mode amplitude range dependence. The phenomenon of nonlinear ray-medium resonance that plays a crucial role in the emergence of ray chaos is shown to have an analog for modes which we call the mode-medium resonance.[61] According to the heuristic criterion proposed by Chirikov,[20–22] chaos is a result of an overlap of different resonances. In terms of normal modes, chaos is shown to result from overlapping mode-medium resonances leading to complicated and irregular range variations of the modal structure.

The normal mode representation of the solution to the parabolic wave equation (17) is obtained by expanding $\Psi(z,r)$ in a sum of eigenfunctions of the unperturbed Sturm–Liouville eigenvalue problem,[63,64]

$$-\frac{1}{2}\frac{d^2\psi_m}{dz^2}+k_0^2 U_0(z)\psi_m=k_0^2 E_m\psi_m, \tag{41}$$

where ψ_m and E_m are the eigenfunctions and eigenvalues, respectively:

$$\Psi(z,r)=\sum_m B_m(r)\psi_m(z). \tag{42}$$

Here it is assumed that $U(z,r)=U_0(z)+\varepsilon V(z,r)$. Each term in the sum (42) represents a contribution from an individual normal mode. In order to get simple semiclassical expressions for the amplitudes, B_m, we project the ray representation of $\Psi(z,r)$ of the form of Eq. (3) onto the normal modes. Assuming the latter to be normalized in such a way that

$$\int_{-\infty}^{\infty} dz\ \psi_m(z)\psi_n(z)=\delta_{mn}, \tag{43}$$

we need to evaluate the integrals

$$B_m(r)=\int_{-\infty}^{\infty} dz\,\Psi(z,r)\psi_m(z). \tag{44}$$

Since we consider the geometric approximation to $\Psi(z,r)$, it is natural to use the same approximation for $\psi_m(z)$. The corresponding formulas are usually referred to as the WKB approximations to the eigenfunctions.[57,63,64]

We shall assume that the potential $U_0(z)$ is smooth, has only one minimum, and its walls tend to infinity as $z \to \pm\infty$. When this assumption is combined with use of the WKB approximation, the eigenvalues of the action variable I_m are determined by the quantization rule

$$k_0 I_m = m + \tfrac{1}{2}. \tag{45}$$

Then the eigenvalues of the "energy" are given by the relation $E_m = E(I_m)$, where the function $E(I)$ is determined by Eq. (21). In the same approximation the mth eigenfunction $\psi_m(z)$ between its turning points can be represented as[57,64]

$$\psi_m(z)=\psi_m^+(z)+\psi_m^-(z), \tag{46}$$

with

$$\psi_m^{\pm}(z)=Q_m(z) \times\exp\left[\pm i\left(k_0\int_{\check{z}}^{z} dz'\,\sqrt{2[E_m-U_0(z')]}-\frac{\pi}{4}\right)\right], \tag{47}$$

$$Q_m(z)=\frac{1}{\sqrt{R_m}[2(E_m-U_0(z)]^{1/4}}, \tag{48}$$

where R_m is the cycle length of the ray in the unperturbed waveguide with $E=E_m$. In this form the eigenfunction is represented as a sum of two terms with rapidly varying phases and slowly varying amplitudes. Substituting Eqs. (46) and the ray representation of $\Psi(z,r)$ of the form (3) into Eq. (44) yields a sum of integrals which can be approximately evaluated by applying the stationary phase technique.[57] This has been done in Ref. 61. Earlier, a related result was obtained in Ref. 65. Here we present only the final expressions for B_m.

The amplitude of the mth mode at the given range r is formed by contributions from the rays whose action values are equal to that of the given mode, i.e., with

$$I=I_m. \tag{49}$$

Here I_m is defined in (45); that expression is used because the normal modes in the background environment are being used as a set of basis functions. Phase space is foliated by surfaces of constant I, defined in the background environment, so at each range, each ray falls onto one of these surfaces. Thus I on the left side of (49) may be considered as a function of range and the initial ray phase space coordinates, i.e.,

$$I=I(p_0,z_0,r). \tag{50}$$

This function is determined by the solutions to Eqs. (9) and (19), and Eq. (21). For a point source the value of z_0 is the same for all rays; substitution of Eq. (50) into Eq. (49) then yields an equation for p_0, whose solutions define the initial momenta of the rays that contribute to the mth mode. We shall refer to these as the eigenrays of the mth mode.

The process of identifying modal eigenrays is illustrated in the right panel of Fig. 2. Two curves are plotted: a surface of constant I and a segment of a Lagrangian manifold. The Lagrangian manifold corresponds, at $r=0$, to a small angular aperture point source. Each intersection of the two curves corresponds to a modal eigenray. Eleven such intersections are shown. Under chaotic conditions this number can grow exponentially in range. (In contrast, in all range-independent environments there are two modal eigenrays for each mode, independent of range, whose launch angles have opposite sign.)

The mode amplitude is given by the sum

$$B_m=\sum_n \frac{1}{\sqrt{k_0|\partial I/\partial p_0|_{p_0=p_{0n}}}} e^{ik_0\Phi_n+i\beta_n}, \tag{51}$$

where each term represents a contribution from an eigenray with an initial momentum p_{0n}. The explicit expressions for the phase terms are (since the subsequent formulas describe characteristics of a single eigenray, the subscript n is omitted)

$$\Phi=S-S_0(z,I_m)\mathrm{sgn}(p) \tag{52}$$

and

$$\beta=\left(\mathrm{sgn}\left(\frac{\partial p/\partial p_0}{\partial z/\partial p_0}\right)-\mathrm{sgn}(p)-2\mu\right)\frac{\pi}{4}. \tag{53}$$

Here z is the depth and p is the momentum of the eigenray at a range r, where S and μ are its eikonal and Maslov index, respectively.

Equations (50)–(53) provide the analytical description of mode amplitudes in a range-dependent environment through the parameters of ray trajectories, i.e., through solutions to the Hamilton equations (9). These equations reduce the mode amplitude evaluation to a procedure quite analogous to that generally used when evaluating the field amplitude at the given point. This involves solving the Hamilton (ray) equations, finding the eigenrays, and calculating ray eikonals and some derivatives with respect to initial values of ray parameters. An important point should be stressed. Although we expand the wave field using eigenfunctions of the unperturbed waveguide, smallness of the perturbation has not been assumed. Our small parameter is the acoustic wavelength, $2\pi/k$, that should be substantially smaller than any physical scale in the problem.

Having the comparatively simple expressions relating the mode amplitudes to rays, we can now discuss how the complicated ray trajectory dynamics reveals itself in the mode amplitude variations. For simplicity, we restrict our attention to a waveguide with a weak (ε is now considered as a small parameter) periodic range dependence with a spatial period $2\pi/\Omega$, and we consider the case when only one mode is excited at $r=0$, i.e.,

$$u(0,z)=\psi_m(z). \tag{54}$$

Analysis of the ray structure for this type of distributed source (see Refs. 61 and 62) shows that for all rays initial values of the action variable I are equal to I_m. A situation which we call *mode-medium resonance* occurs when the value of I_m satisfies Eq. (24). Due to the resonance, at ranges of order of $1/\Delta\omega$ there will appear a bundle of rays with the action variables I in the interval $|I-I_0|<\Delta I_{\max}$. Here I_0 is the action value of the resonant ray. This means [see Eq. (49)] that starting with such ranges, the mth mode is split into a group of $2M$ modes with

$$M=\Delta I_{\max}/k_0=2\sqrt{\varepsilon\overline{V}/|\omega'|}/k_0, \tag{55}$$

where $\overline{V}$ is the magnitude of the perturbation potential V. This expression is the modal analog of the standard expression [Eq. (25)] for the width of a ray resonance. In the case of overlapping modal resonances it is natural to expect a further broadening of a group of modes. Moreover, as we discussed earlier, the overlapping of resonances causes the emergence of ray chaos with exponential proliferation of eigenrays. Under chaotic conditions the number of eigenrays contributing to a given mode also grows exponentially with range, giving rise to a very complicated range dependence of mode amplitudes. Numerical simulations presented in Refs. 61 and 62 support these statements.

It might be assumed that that exponential proliferation of eigenrays contributing to a given mode leads to statistical independence of mode amplitude fluctuations under chaotic conditions. We expect, however, that the problem of describing mode amplitudes is considerably more rich and complicated. First, it should be recalled that generically the phase space of a chaotic Hamiltonian system contains both chaotic regions and ''stable islands'' formed by regular periodic trajectories. Some such regular rays will be eigenrays for some modes. Their contributions to modes cannot be considered as stochastic. Thus, we expect that under chaotic conditions there will be modes with amplitudes composed of two constituents: a chaotic one and a regular one. Numerical results illustrating this statement have been presented in Ref. 62. Another important phenomenon typical of chaotic dynamics, which may affect modal structure variations is stickiness, i.e., the presence of segments of a chaotic trajectory which exhibit almost regular behavior. The interval over which apparently regular behavior is observed can be long. In principle, one can presume that stickiness may cause some long-lasting correlations of mode amplitudes.[43]

Our ray-based description of normal mode amplitudes has restrictions that are very much like those of standard ray theory. In particular, at some points the contribution from an eigenray to a given mode can be infinite. This occurs when the derivative in the denominator in Eq. (51) vanishes. [The same comment applies to Eq. (59) below.] Such divergences represent analogs of standard ray theory caustics. Under conditions of ray chaos the number of such caustics grows exponentially with range, spoiling applicability of the ray-based description already at short distances. This issue is discussed in Ref. 62. On the other hand, in Ref. 62 (see also Ref. 49) it was demonstrated numerically that the approach considered in this section can properly predict squared mode amplitudes smoothed over the mode number at ranges of order of at least ten inverse Lyapunov exponents. This result is rather encouraging. It gives us hope that energy redistribution between modes can be comparatively easily analyzed using simple ray calculations at ranges of the order of a few thousand km.

So far, we have considered only a cw field. For a signal with a finite bandwidth, the mode sum must include an integration over frequency σ. The pulse signal at the point (z,r) can be represented as

$$u(z,r,t)=\sum_m u_m(z,r,t), \tag{56}$$

where

$$u_m(z,r,t)=\int d\sigma\, s(\sigma)B_m(r,\sigma)\psi_m(z,\sigma)e^{i\sigma(r/c_0-t)} \tag{57}$$

with $s(\sigma)$ being the spectrum of the initially radiated pulse. In Eq. (57) we have indicated explicitly the dependence of B_m and ψ_m on σ, which has been omitted until now. Each term, $u_m(z,r,t)$, in the sum (56) can be interpreted as a pulse carried by an individual mode and we shall call it the ''mode'' pulse. The mode pulse, in turn, can be regarded as a superposition of elementary pulses representing contributions from different terms in the sum (51):

$$u_m(z,r,t)=\sum_n \int d\sigma\, s(\sigma)G_m(z,r,\sigma)e^{i\sigma((\Phi_n+r)/c_0-t)}, \tag{58}$$

where

$$G_m(z,r,\sigma)=\frac{e^{i\beta_n}}{\sqrt{k_0 r|\partial I/\partial p_0|_{p_0=p_{0n}}}} \times\frac{2\cos(k_0\int_z^z dz'\sqrt{2[E_m-U_0(z')]}-\pi/4)}{\sqrt{R_m}[2(E_m-U_0(z)]^{1/4}}. \tag{59}$$

The above expressions depend on mode parameters with the subscript m and eigenray parameters with the subscript n. Note that both types of parameters depend on frequency. Although the trajectories of eigenrays contributing to the given mode obey frequency-independent Hamilton equations (9), their starting momenta determined by Eq. (49) depend on the eigenvalue I_m. But the latter, according to Eq. (45), does depend on frequency. Under chaotic conditions the number of terms in Eq. (58) can be huge, leading to a very complicated shape of the mode pulse.

The expectation that mode pulses are very complicated under chaotic conditions is consistent with the numerical results in Ref. 66, where broadband parabolic-equation simulations of sound transmission through a deep water acoustic waveguide with inhomogeneities induced by random internal waves are described. It was shown that, due to mode coupling, mode pulses were several times longer than was the case in the background range-independent environment, and acquired irregular shapes. In contrast, from the ray perspective, the same weak inhomogeneities caused steep eigenrays to split into clusters of eigenrays (micromultipaths) whose

travel time spreads were small and whose centroid had a travel time that was close to that of the eigenray in the background environment. (Recall also Sec. III of the present paper.) The authors of Ref. 66 concluded that ''while the high modes may be strongly affected by internal waves they are coherent enough that when they are synthesized together localized wave front results.'' A qualitative explanation of this phenomenon has been offered in Ref. 67. In that paper it was shown that mode pulses may be considerably distorted due to mode coupling already at ranges so short that chaotic ray dynamics has not yet had a chance to reveal itself and every mode is formed by contributions from only two eigenrays. It was also demonstrated how distorted pulses carried by individual modes can combine to produce much less distorted raylike pulses at the receiver.

Although the mode coupling relations presented above are not easy to test experimentally, we emphasize that these results are important because of the insight they provide into the underlying propagation physics. In this regard, it should be noted that the mode coupling relations presented above directly address the connection between ray chaos and finite frequency propagation effects, i.e., the wave chaos problem.

VII. DISCUSSION

In this paper we have reviewed results relating to ray dynamics in ocean acoustics. All of these results are intimately linked to the Hamiltonian structure of the ray equations. Most previous studies have emphasized the applicability of KAM theory to oceans with periodic range dependence and the extreme sensitivity of individual chaotic ray trajectories. To complement these ideas, considerable attention has been focused on oceans with nonperiodic range dependence, and we have discussed some forms of stability of distributions of chaotic rays. Also, we have discussed subjects such as nondegeneracy violation, ray intensity statistics, and the connection between ray chaos and mode coupling that either have not, or have only recently, been explored in an underwater acoustic context.

Although our understanding of ray dynamics is currently incomplete, it should be clear that the most pressing problem in this context is to better understand the connection between the ray dynamics and the corresponding finite frequency wave fields. For example, even the seemingly simple task of translating ray intensity statistics to wave field intensity statistics is complicated by the necessity of making an additional assumption about relative phases and correcting for diffractive effects.

It is our hope that the theoretical results presented in this paper provide a foundation for the analysis of measurements of sound fields at long range in the deep ocean. An analysis of this type will be presented in a forthcoming paper. Our long-term goal of developing tools that can be used to assist in the analysis of measurements accounts, in large part, for the considerable attention that we have devoted to ocean structures with nonperiodic range dependence.

The ideas and results that we have discussed differ in some important respects from more commonly applied ideas and results associated with the study of wave propagation in random media (WPRM). For example, in the deterministic chaos point of view, the excitation of ray-medium resonances generally leads to a mixed phase space. Most approaches to WPRM, on the other hand, invoke the assumption that the perturbation to the background sound speed structure is delta-correlated; this leads to stochasticity, but not to a mixed phase space. Also, most long-range underwater acoustic propagation WPRM theories (see, e.g., Ref. 68) assume that stochasticity is caused exclusively by internal waves. From the deterministic chaos point of view, this assumption is difficult to justify inasmuch as non-internal-wave (e.g., mesoscale) structure may excite ray-medium resonances and chaos. Although we have argued that a traditional WPRM framework is a good starting point for some purposes, such as understanding ray intensity statistics, it is unable to provide an explanation for other phenomena that we have described such as the connection between ray stability and ω'. We anticipate that, over the next decade or so, ideas relating to deterministic chaos will gradually be incorporated into theories of WPRM.

Finally, we wish to remark that the importance of ray methods is not diminished by recent advances, both theoretical and computational, in the development of full wave models, such as those based on parabolic equations. The latter are indispensible computational tools in many applications. In contrast, the principal virtue of ray methods is that they provide insight into the underlying wave physics that is difficult, if not impossible, to obtain by any other means. For this reason ray methods remain important.

ACKNOWLEDGMENTS

We thank F. Tappert and F. J. Beron-Vera for the benefit of discussions on many of the topics included in this paper. This work was supported by Code 321 OA of the U.S. Office of Naval Research.

[1] S. S. Abdullaev and G. M. Zaslavsky, ''Stochastic instability of rays and the speckle structure of the field in inhomogeneous media,'' Zh. Eksp. Teor. Fiz. **87**, 763–775 (1984) [Sov. Phys. JETP **60**, 435–441 (1985)].
[2] D. R. Palmer, M. G. Brown, F. D. Tappert, and H. F. Bezdek, ''Classical chaos in nonseparable wave propagation problems,'' Geophys. Res. Lett. **15**, 569–572 (1988).
[3] S. S. Abdullaev and G. M. Zaslavsky, ''Fractals and ray dynamics in longitudinally inhomogeneous media,'' Sov. Phys. Acoust. **34**, 334–336 (1989).
[4] S. S. Abdullaev and G. M. Zaslavskii, ''Classical nonlinear dynamics and chaos of rays in wave propagation problems in inhomogeneous media,'' Usp. Phys. Nauk **161**, 1–43 (1991).
[5] M. G. Brown, F. D. Tappert, and G. Goñi, ''An investigation of sound ray dynamics in the ocean volume using an area-preserving mapping,'' Wave Motion **14**, 93–99 (1991).
[6] F. D. Tappert, M. G. Brown, and G. Goñi, ''Weak chaos in an area-preserving mapping for sound ray propagation,'' Phys. Lett. A **153**, 181–185 (1991).
[7] M. G. Brown, F. D. Tappert, G. Goñi, and K. B. Smith, ''Chaos in underwater acoustics,'' in *Ocean Variability and Acoustic Propagation*, edited by J. Potter and A. Warn-Varnas (Kluwer Academic, Dordrecht, 1991), pp. 139–160.
[8] D. R. Palmer, T. M. Georges, and R. M. Jones, ''Classical chaos and the sensitivity of the acoustic field to small-scale ocean structure,'' Comput. Phys. Commun. **65**, 219–223 (1991).
[9] K. B. Smith, M. G. Brown, and F. D. Tappert, ''Ray chaos in underwater acoustics,'' J. Acoust. Soc. Am. **91**, 1939–1949 (1992).
[10] K. B. Smith, M. G. Brown, and F. D. Tappert, ''Acoustic ray chaos induced by mesocsale ocean structure,'' J. Acoust. Soc. Am. **91**, 1950–1959 (1992).

[11] S. S. Abdullaev, *Chaos and Dynamics of Rays in Waveguide Media*, edited by G. Zaslavsky (Gordon and Breach Science, New York, 1993).
[12] F. D. Tappert and X. Tang, ''Ray chaos and eigenrays,'' J. Acoust. Soc. Am. **99**, 185–195 (1996).
[13] G. M. Zaslavsky and S. S. Abdullaev, ''Chaotic transmission of waves and 'cooling' of signals,'' Chaos **7**, 182–186 (1997).
[14] J. Simmen, S. M. Flatté, and G.-Yu Wang, ''Wavefront folding, chaos and diffraction for sound propagation through ocean internal waves,'' J. Acoust. Soc. Am. **102**, 239–255 (1997).
[15] M. Wiercigroch, M. Badiey, J. Simmen, and A. H.-D. Cheng, ''Nonlinear dynamics of underwater acoustics,'' J. Sound Vib. **220**, 771–786 (1999).
[16] M. A. Wolfson and F. D. Tappert, ''Study of horizontal multipaths and ray chaos due to ocean mesoscale structure,'' J. Acoust. Soc. Am. **107**, 154–162 (2000).
[17] M. A. Wolfson and S. Tomsovic, ''On the stability of long-range sound propagation through a structured ocean,'' J. Acoust. Soc. Am. **109**, 2693 (2001).
[18] U. Eichman, K. Richter, D. Wintgen, and W. Sandner, ''Scaled energy spectroscopy and its relation with periodic orbits,'' Phys. Rev. Lett. **61**, 2438–2441 (1988).
[19] L. D. Landau and E. M. Lifshits, *Mechanics* (Nauka, Moscow, 1973).
[20] B. V. Chirikov, ''A universal instability of many-dimensional oscillator systems,'' Phys. Rep. **52**, 263–379 (1979).
[21] G. M. Zaslavsky and B. V. Chirikov, ''Stochastic instability of non-linear oscillations,'' Sov. Phys. Usp. **14**, 549–672 (1972).
[22] A. G. Lichtenberg and M. A. Lieberman, *Regular and Stochastic Motion* (Springer Verlag, New York, 1983).
[23] M. Tabor, *Chaos and Integrability in Nonlinear Dynamics* (Wiley-Interscience, New York, 1989).
[24] M. G. Brown, ''Phase space structure and fractal trajectories in 1 1/2 degree of freedom Hamiltonian systems whose time dependence is quasi-periodic,'' Nonlinear Process. Geophys. **5**, 69–74 (1998).
[25] J. A. Colosi and M. G. Brown, ''Efficient numerical simulation of stochastic internal-wave-induced sound speed perturbation fields,'' J. Acoust. Soc. Am. **103**, 2232–2235 (1998).
[26] G. M. Zaslavsky, M. Edelman, and B. A. Niyazov, ''Self-similarity, renormalization and phase nonuniformity of Hamiltonian chaotic dynamics,'' Chaos **7**, 159–181 (1997).
[27] E. Ott, *Chaos in Dynamical Systems* (Cambridge U. P., Cambridge, 1993).
[28] P. Gaspard and G. Nicolis, ''Transport properties, Lyapunov exponents, and entropy per unit time,'' Phys. Rev. Lett. **65**, 1693–1696 (1990).
[29] N. R. Cerruti and S. Tomsovic, ''Sensitivity of wave field evolution and manifold stability in chaotic systems,'' Phys. Rev. Lett. **88**, 054103 (2002); nlin.CD/0108016.
[30] W. H. Munk, ''Sound channel in an exponentially stratified ocean with application to SOFAR,'' J. Acoust. Soc. Am. **55**, 220–226 (1974).
[31] A. A. Chernikov, R. Z. Sagdeev, and G. M. Zaslavsky, ''Chaos: How regular can it be?'' Phys. Today **41**, 27–35 (1988).
[32] G. M. Zaslavsky, *Physics of Chaos in Hamiltonian Systems* (Imperial College, London, 1998).
[33] F. J. Beron-Vera and M. G. Brown, ''Ray stability in weakly range-dependent sound channels,'' J. Acoust. Soc. Am. (in press).
[34] T. F. Duda and J. B. Bowlin, ''Ray acoustic caustic formation and timing effects from ocean sound speed relative curvature,'' J. Acoust. Soc. Am. **96**, 1033–1046 (1994).
[35] V. I. Shishov, ''Theory of wave propagation in random media,'' Izv. Vyssh. Uchebn. Zaved., Radiofiz. **11**, 866–875 (1968).
[36] G. Hasinger, R. Giacconi, J. E. Gunn, I. Lehmann, M. Schmidt, D. P. Schneider, J. Trümper, J. Wambsganss, D. Woods, and G. Zamorani, ''The ROSAT Deep Survey IV. A distant lensing cluster of galaxies with a bright arc,'' Astron. Astrophys. **340**, L27–L30 (1998).
[37] *Mesoscopic Quantum Physics*, edited by E. Akkermans, G. Montambaux, J.-L. Pichard, and J. Zinn-Justin, Les Houches Session LXI, 1994 (Elsevier Science, Amsterdam, 1995).
[38] M. A. Topinka, B. J. LeRoy, R. M. Westervelt, S. E. J. Shaw, R. Fleischmann, E. J. Heller, K. D. Maranowski, and A. C. Gossard, ''Coherent branched flow in a two-dimensional electron gas,'' Nature (London) **410**, 183 (2001).
[39] M. V. Berry, ''Focusing and twinkling: critical exponents from catastophes in non-Gaussian random short waves,'' J. Phys. A **10**, 2061–2081 (1977).
[40] J. G. Walker, M. V. Berry, and C. Upstill, ''Measurements of twinkling exponents of light focused by randomly rippling water,'' Opt. Acta **30**, 1001–1010 (1983).
[41] J. H. Hannay, ''Intensity fluctuations beyond a one-dimensional random refracting screen in the short-wavelength limit,'' Opt. Acta **29**, 1631–1649 (1982).
[42] E. J. Heller and S. Tomsovic, ''Postmodern Quantum Mechanics,'' Phys. Today **46**(7), 38–45 (1993).
[43] B. Sundaram and G. M. Zaslavsky, ''Wave analysis of ray chaos in underwater acoustics,'' Chaos **9**, 483–492 (1999).
[44] *Quantum Chaos: between Order and Disorder: a Selection of Papers*, edited by G. Casati and B. V. Chirikov (Cambridge U. P., New York, 1995).
[45] *Chaos and Quantum Physics*, edited by M. J. Giannoni, A. Voros, and J. Zinn-Justin, Les Houches Session LII, 1989 (Elsevier Science, Amsterdam, 1991).
[46] G. M. Zaslavsky, ''Stochasticity in quantum systems,'' Phys. Rep. **80**, 157–250 (1980).
[47] N. L. Balazs and B. K. Jennings, ''Wigner function and other distribution functions in mock phase spaces,'' Phys. Rep. **104**, 347–391 (1984).
[48] D. Bambusi, S. Graffi, and T. Paul, ''Long time semiclassical approximation of quantum flows: A proof of the Ehrenfest time,'' Asymptotic Anal. **21**, 149–160 (1999).
[49] A. L. Virovlyansky and G. M. Zaslavsky, ''Evaluation of the smoothed interference pattern under conditions of ray chaos,'' Chaos **10**, 211–223 (2000).
[50] P. W. O'Connor, S. Tomsovic, and E. J. Heller, ''Semiclassical Dynamics in the Strongly Chaotic Regime: Breaking the Log Time Barrier,'' Physica D **55**, 340 (1992).
[51] M.-A. Sepulveda, S. Tomsovic, and E. J. Heller, ''Semiclassical propagation: How long can it last?'' Phys. Rev. Lett. **69**, 402–405 (1992).
[52] S. Tomsovic and E. J. Heller, ''Long-time semiclassical dynamics of chaos: The stadium billiard,'' Phys. Rev. E **47**, 282–299 (1993).
[53] M. D. Collins and J. F. Lingevitch, ''Secular behavior and breakdown of chaotic ray solutions,'' IEEE J. Ocean. Eng. **22**, 102–109 (1997).
[54] M. G. Brown and M. A. Wolfson, ''A numerical investigation of semiclassical breakdown in an idealized random medium,'' in preparation (2002).
[55] L. B. Felsen, ''Hybrid ray-mode fields in inhomogeneous waveguides and ducts,'' J. Acoust. Soc. Am. **62**, 352–361 (1981).
[56] T. Gao and E. C. Shang, ''The transformation between the mode representation and the generalized ray representation of a sound field,'' J. Sound Vib. **80**, 105–115 (1982).
[57] L. M. Brekhovskikh and Yu. Lysanov, *Fundamentals of Ocean Acoustics* (Springer-Verlag, Berlin, 1991).
[58] A. L. Virovlyansky, V. V. Kurin, N. V. Pronchatov-Rubtsov, and S. I. Simdyankin, ''Fresnel zones for modes,'' J. Acoust. Soc. Am. **101**, 163–173 (1997).
[59] A. L. Virovlyanskii and A. G. Kosterin, ''Method of smooth perturbations for the description of the fields in multimode waveguides,'' Sov. Phys. Acoust. **33**, 351–354 (1987).
[60] A. L. Virovlyansky, A. G. Kosterin, and A. N. Malakhov, ''Fresnel zones for modes and analysis of field fluctuations in random multimode waveguides,'' Waves Random Media **1**, 409–418 (1991).
[61] A. L. Virovlyansky and G. M. Zaslavsky, ''Wave chaos in terms of normal modes,'' Phys. Rev. E **59**, 1656–1668 (1999).
[62] A. L. Virovlyansky, ''Manifestation of ray stochastic behavior in a modal structure of the wave field,'' J. Acoust. Soc. Am. **108**, 84–95 (2000).
[63] L. D. Landau and E. M. Lifshits, *Quantum Mechanics* (Moscow, Nauka, 1974).
[64] F. B. Jensen, W. A. Kuperman, M. B. Porter, and H. Schmidt, *Computational Ocean Acoustics* (American Institute of Physics, New York, 1994).
[65] G. P. Berman and G. M. Zaslavsky, ''Condition of stochasicity in quantum nonlinear systems,'' Physica A **97**, 367–382 (1979).
[66] J. A. Colosi and S. M. Flatté, ''Mode coupling by internal waves for multimegameter acoustic propagation in the ocean,'' J. Acoust. Soc. Am. **100**, 3607–3620 (1996).
[67] A. L. Virovlyansky, ''Comments on 'Mode coupling by internal waves for multimegameter acoustic propagation in the ocean' [J. Acoust. Soc. Am. **100**(6), 3607–3620 (1996)],'' J. Acoust. Soc. Am. **106**, 1174–1176 (1999).
[68] S. Flatté, R. Dashen, W. Munk, K. Watson, and F. Zachariasen, *Sound Transmission through a Fluctuating Ocean* (Cambridge U.P., Cambridge, 1979).